We are IntechOpen,
the world's leading publisher of Open Access books
Built by scientists, for scientists

6,600
Open access books available

178,000
International authors and editors

195M
Downloads

154
Countries delivered to

Our authors are among the

TOP 1%
most cited scientists

12.2%
Contributors from top 500 universities

WEB OF SCIENCE™

Selection of our books indexed in the Book Citation Index
in Web of Science™ Core Collection (BKCI)

Interested in publishing with us?
Contact book.department@intechopen.com

Numbers displayed above are based on latest data collected.
For more information visit www.intechopen.com

Localization Techniques in Multiple-Input Multiple-Output Communication: Fundamental Principles, Challenges, and Opportunities

Katarina Vuckovic and Nazanin Rahanvard

Abstract

This chapter provides an overview of localization techniques in Multiple-Input Multiple-Output (MIMO) communication systems. The chapter mainly focuses on sub-6 GHz and mmWave bands. MIMO technology enables high-capacity wireless communication, but also presents challenges for localization due to the complexity of the signal propagation environment. Various methods have been developed to overcome these challenges, which utilize side information such as the map of the area, or techniques such as Compressive Sensing (CS), Deep Learning (DL), Gaussian Process Regression (GPR), or clustering. These techniques utilize wireless communication parameters such as Received Signal Strength Indicator (RSSI), Channel State Information (CSI), Angle-Delay-Profile (ADP), Angle-of-Departure (AoD), Angle-of-Arrival (AoA), or Time-of-Arrival (ToA) as inputs to estimate the user's location. The goal of this chapter is to offer a comprehensive understanding of MIMO localization techniques, along with an overview of the challenges and opportunities associated with them. Furthermore, it also aims to provide the theoretical background on channel models and wireless channel parameters required to understand the localization techniques.

Keywords: localization techniques, positioning system, channel model, channel parameters, machine learning

1. Introduction

The proliferation of smartphone devices has enabled the expansion of Location Based Services (LBS) [1]. With the increasing popularity of LBS applications, there is a growing demand for more accurate localization solutions. Wireless MIMO localization is an alternative solution to the widely accepted Global Positioning System (GPS) in environments where GPS falls short. Specifically, GPS faces a challenge in maintaining accuracy and availability with urban canyons and indoor environments

[2]. Wireless MIMO systems already exist in these environments for communication purposes. Therefore, the existing wireless communication infrastructure can also be leveraged to provide localization services without investing in additional equipment. In fact, many LBS applications are enabled by wireless MIMO localization. While compiling a comprehensive list of these applications would be difficult, the following subsections provide an overview of some interesting LBS applications.

1.1 Applications

1.1.1 Emergency services

The purpose of emergency services is to identify a caller's location and provide this information to the emergency responders. Emergency service is the oldest LBS application. The need to position mobile users was first advocated back in 1996 when the Federal Communication Commission (FCC) announced its mandate to enhance emergency services. During that time, the main motivation was mostly centered around locating emergency calls [3]. Since then, both FCC Enhanced 911 (E911) and 3rd Generation Partnership Project (3GPP) requirements for localization accuracy have become more stringent [4, 5].

1.1.2 Autonomous vehicles and urban air mobility

Precise positioning systems play a crucial role in autonomous vehicles and Unmanned Aerial Systems (UASs) [6]. The purpose of these positioning systems is to provide accurate estimations of the vehicle's location and orientation relative to the road and other vehicles (whether terrestrial or aerial). Moreover, the localization systems facilitate tracking of other vehicles, pedestrians, and obstacles in the surroundings. This information is utilized to plan safe and efficient routes, and to avoid collisions. The wireless MIMO system can provide primary location estimation or a backup in the event of GPS failure or loss of other proximity sensors [2]. Several studies have explored using MIMO localization for vehicles [7–11] and UASs [12–14].

1.1.3 Field surveying and mapping

Field surveying and mapping has both civilian and military applications including creating detailed topographical maps, measuring land boundaries, and collecting data on natural resources. For example, in construction surveying, positioning and localization systems are used to ensure that buildings and infrastructures are positioned and aligned correctly. In military applications, these systems can be used for reconnaissance of enemy territory and targeting of enemy or enemy assets. Simultaneous Localization and Mapping (SLAM) is often employed in these types of applications. SLAM is an active area of research and over the past few years, various surveys have been published that summarize the state-of-the-art SLAM solutions [15–17].

1.1.4 Indoor tracking and localization

Indoor tracking and localization technology have numerous practical applications across various industries. In healthcare, it can be used to track the location of medical

equipment, staff and patients, ensuring efficient use of resources and timely delivery of care [18]. In the retail industry, it can help to optimize store layouts and improve the customer experience by providing personalized recommendations and targeted advertising. In industrial settings, it can improve warehouse logistics and inventory management by providing real-time tracking of goods and equipment [19]. Additionally, indoor tracking and localization can be used to enhance the safety of buildings and occupants by detecting and responding to emergencies, such as fires or security breaches. The technology also has potential applications in the field of smart architectures (smart homes [20], smart buildings [21], smart cities [22], and smart grids [23]) where it can be used to automate and optimize tasks and energy consumption.

1.1.5 Agriculture

Highly accurate localization systems have a wide range of applications in agriculture, including precision farming, autonomous equipment, livestock tracking, and soil mapping [24–28]. In precision farming, localization systems are used to collect data on soil conditions, crop growth, weather patterns, and other factors, which can then be analyzed to make informed decisions about crop management, including planting, fertilization, irrigation, and harvesting. Moreover, the accurate localization systems are also used to guide autonomous equipment to carry out tasks such as planting, spraying, and harvesting with greater precision and efficiency.

1.1.6 Social networking

LBS-enabled social networking applications aim to connect people who are located near each other and share similar interests. These applications use location data to recommend nearby events, activities, or groups that users might be interested in, and facilitate connections with others who are nearby. This approach offers benefits for both individuals and businesses. Some popular LBS-enabled social networking applications include Meetup, Foursquare, Yelp, and Facebook Places.

2. Wireless MIMO system

2.1 Sub-6 GHz and mmWave massive MIMO systems

Fifth-Generation and Beyond (5G&B) mobile networks offer the potential for significantly greater communication capacity and ultra high-speeds that exceed those of previous generations by several orders of magnitude [29]. The large number of antennas in massive MIMO allows for more precise control of the signals, leading to increased capacity, better coverage, improved energy efficiency and reliability [30, 31]. Specifically, massive MIMO antennas enable the generation of narrow and highly directional signal beams. A beam can be steered towards a user to provide a high-quality signal that is less susceptible to interference and fading.

Sub-6 GHz bands are typically between 1 and 6 GHz. This frequency range is commonly used for wireless communication technologies such as cellular networks (3G, 4G, and 5G), Wi-Fi, Bluetooth, and other wireless communication standards. Sub-6 GHz systems are typically implemented using small-scale MIMO antennas. Regarding the sub-6 GHz channel, several measurement campaigns have been carried

out to characterize it [32–34]. The propagation that depends on path-loss and shadowing results in large-scale fading, and multi-path propagation, results in small-scale fading [35].

The massive increase in data traffic has made the sub-6 GHz spectrum congested. This results in limited bandwidth for users, causing slower and unreliable connections [36]. One solution to this problem is to move to a different frequency band such as milimeter-Wave (mmWave) frequency channels. The channels are called mmWave because their wavelength ranges between 1 mm and 10 mm, which is equivalent to a frequency range between 30 GHz and 300 GHz. The mmWave channels can provide significantly more bandwidth compared to sub-6 GHz, which will be required for next generation wireless communication systems. Therefore, mmWave frequency has been identified as a key technology-enabler in 5G&B [30, 35, 36]. However, there are some disadvantages in mmWave communication such as severe signal attenuation and blockage. The signals cannot penetrate obstacles and tend to get absorbed by rain [37, 38].

In an experimental study, a comprehensive channel measurement campaign was conducted in Europe in 2014–2016 in numerous indoor and outdoor scenarios. The study showed that geometry of the main propagation paths at sub-6 GHz and mmWave bands are almost similar [39]. However, the blockage at mmWave band causes higher losses, rendering the path completely blocked. This experimental out-come has motivated several recent studies to use sub-6 GHz channel information for mmWave applications [40–42].

2.2 Single-site system model

In wireless communication, the Base Station (BS) and User Equipment (UE) engage in point-to-point communication as shown in **Figure 1**. The BS may function
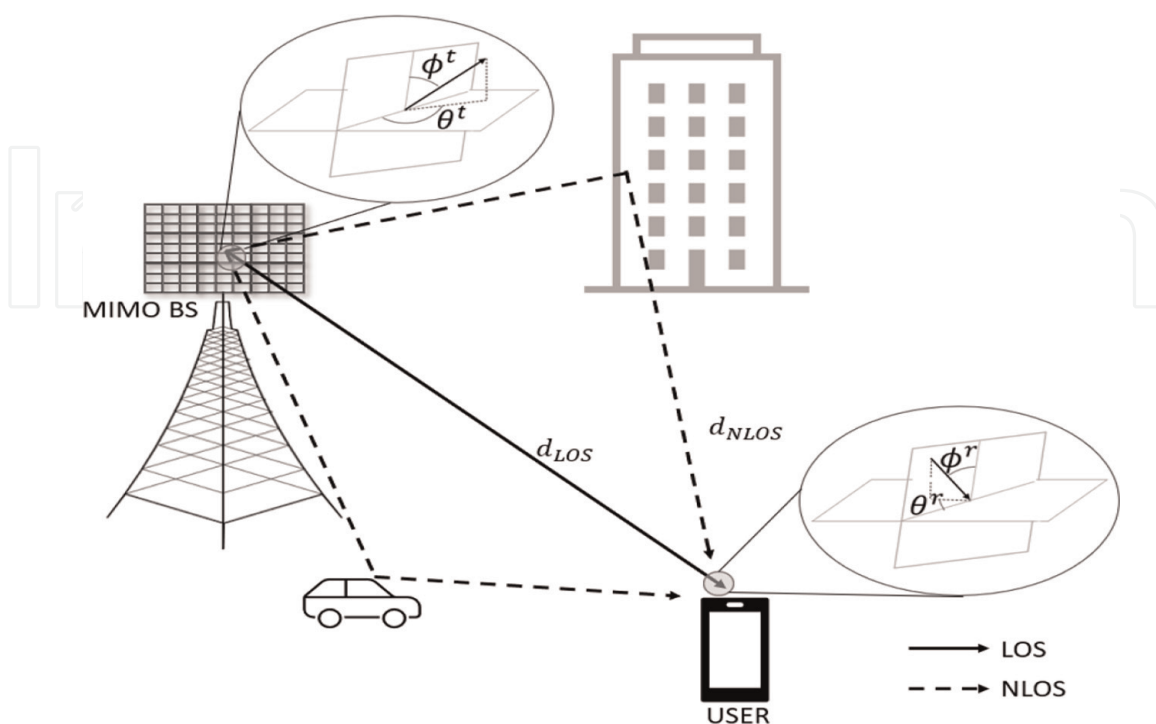

Figure 1.
Single-site wireless MIMO channel model showing LOS and NLOS propagation paths between BS and UE.

as an Access Point (AP) or as another device in device-to-device communication. Typically, the BS has multiple antenna array elements while the UE may have one or more antenna elements. A general assumption is that the BS and UE are located in the far-field zones of each other, and multiple propagation paths exist between them. Multipaths arise from either reflection off objects or scattering [43]. Typically, there is a Line-of-Sight (LOS) path and several Non-LOS (NLOS) paths. The LOS path can be blocked, in which case only NLOS paths may exist.

Regardless of which side transmits the signal, the propagation path geometry between the BS and UE remains the same. Each path is characterized by an Angle-of-Departure (AoD), an Angle-of-Arrival (AoA), a Time-of-Arrival (ToA), and a complex gain. Since the signal geometry is invariant, it is possible to use AoA and AoD interchangeably. The AoD and AoA are vectors that define the azimuth and elevation angles in 3D space, while ToA represents the time it takes for the propagating signal to travel from the transmitter to the receiver. The ToA is sometimes referred to as the propagation path *delay*. ToA is equal to the length of the path traveled (d) divided by the speed of light (c):

$$\tau = d/c. \tag{1}$$

The 2D multipath propagation geometry is illustrated in **Figure 2**. In the LOS case, the shortest distance between the BS and UE represents the path traveled by the LOS signal. Furthermore, **Figure 2(a)** shows the AoD from the BS θ_{LOS}^t and AoA at the UE θ_{LOS}^r. On the other hand, the NLOS propagation path can be modeled using a *virtual BS* (BS') [43] as depicted in **Figure 2(b)**. A NLOS path can be thought of as direct path from a virtual node behind the reflecting surface. The virtual BS is on the opposite side of the reflecting surface, maintaining the same distance from it as the original BS, resulting in $d_{NLOS1} = d'_{NLOS1}$. The total path traveled by the NLOS signal is $d_{NLOS} = d_{NLOS1} + d_{NLOS2}$. Furthermore, the AoD from the virtual BS can be calculated as $\pi - \theta_{NLOS}^t$, where θ_{NLOS}^t is the AoD at the original BS.

2.3 Channel model

The wireless communication community has widely adopted the COST 2100 MIMO channel model [44] as the predominant geometric channel model. This model
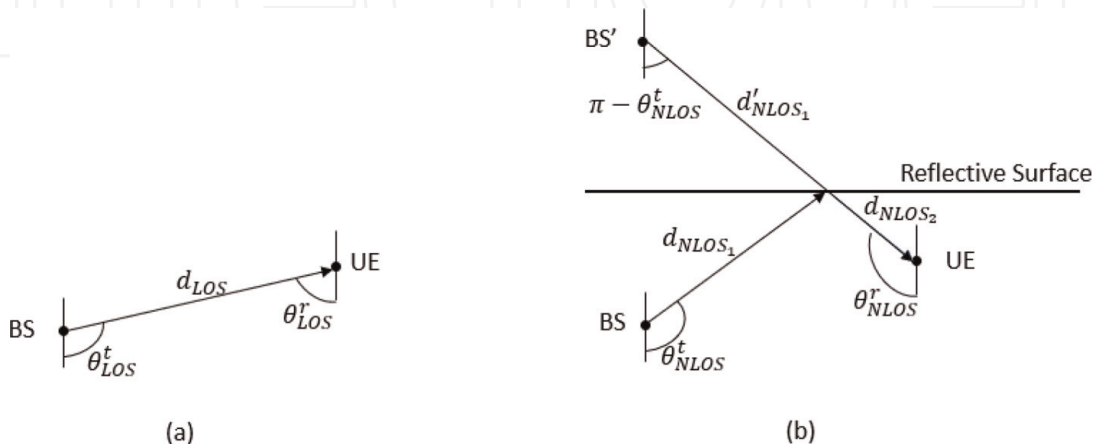

Figure 2.
(a) LOS propagation path geometry for estimating relative location of the UE with respect to the BS. (b) NLOS propagation path and virtual BS (BS') geometry for estimating relative location of the UE with respect to the BS.

5

expresses that a propagation environment can be defined by a set of scatterers that create clusters of multipath components. The model is applicable for both sub-6 GHz and mmWave band frequencies.

Consider a MIMO Orthogonal Frequency-Division Multiplexing (OFDM) wireless system, in which the BS and the UE are equipped with antenna arrays with N_B and N_U elements, respectively. The system uses OFDM signaling with N_C subcarriers and the wideband channel has L taps. The received signal at the lth subcarrier of the UE antenna array can be expressed as

$$\boldsymbol{y}[l] = \boldsymbol{H}[l]\boldsymbol{s}[l] + \boldsymbol{n}[l]. \tag{2}$$

Here, $\boldsymbol{y}[l] \in \mathbb{C}^{N_U \times 1}$ denotes the received signal, $\boldsymbol{H}[l] \in \mathbb{C}^{N_U \times N_B}$ represents the channel matrix, $\boldsymbol{s}[l] \in \mathbb{C}^{N_B \times 1}$ represents the transmitted signal, and $\boldsymbol{n}[l] \sim \mathcal{NC}(\boldsymbol{0}, , \sigma^2 \boldsymbol{I})$ denotes the noise at the receiver.

The propagation paths between the BS and the UE can be split into C distinguishable path clusters, with each cluster containing R_C distinguishable paths. Each path cluster is characterized by a mean time delay $\tau_m^{(k)}, k \in 1, \ldots, C, m \in 1, \ldots, R_C$, a mean AoD $\theta_c^{tx}, \phi_c^{tx} \in [0, \pi)$, and a mean AoA $\theta_c^{rx}, \phi_c^{rx} \in [0, 2\pi)$. Each cluster contributes R_C paths between the transmitter and the receiver, where each path has a relative time delay τ_{c_m} (relative with respect to mean), a relative AOD $\theta_{c_m}^{tx}, \phi_{c_m}^{tx}$, a relative AOA $\theta_{c_m}^{rx}, \phi_{c_m}^{rx}$, and a complex path gain α_{c_m}. The mean and relative paths are illustrated in **Figure 3**.

2.4 Channel state information (CSI)

Assuming the channel model defined above, the complex baseband delay-ℓ MIMO channel matrix $\boldsymbol{H}[\ell] \in \mathbb{C}^{N_U \times N_B}$ can be written as [45, 46]
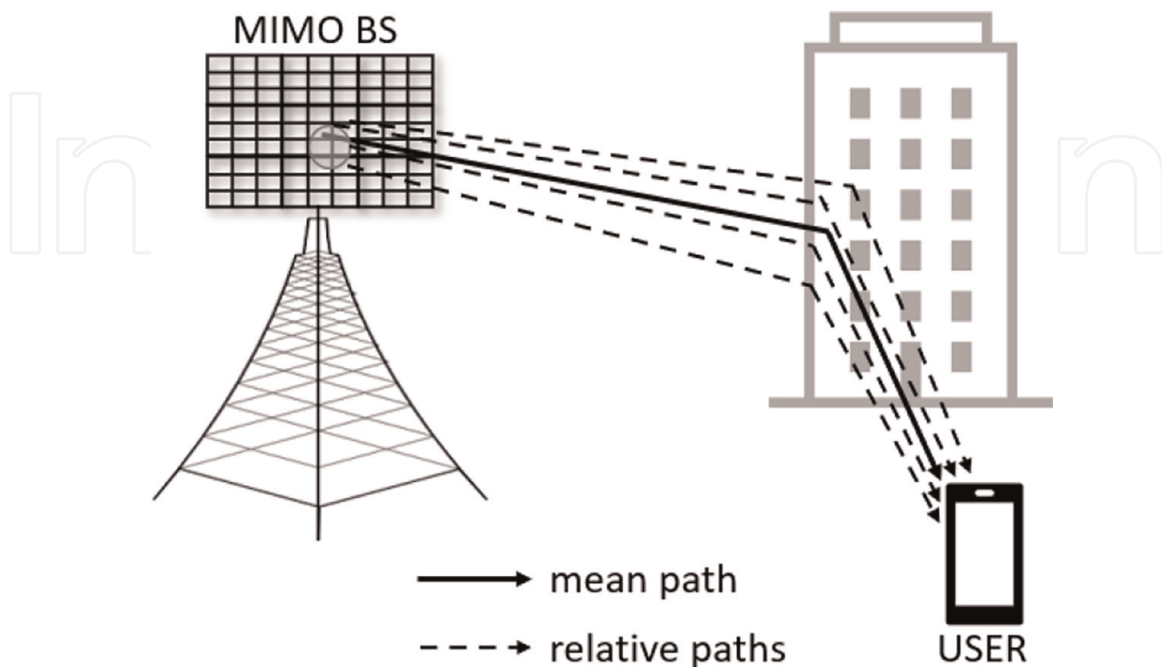

Figure 3.
The mean and relative paths of a NLOS path.

$$\boldsymbol{H}[\ell] = \sqrt{\frac{N_B N_U}{P_{pl}}} \sum_{c=1}^{C} \sum_{c_m=1}^{R_C} \alpha_{c_m} \boldsymbol{e}_{rx}\left(\theta_c^{rx} + \theta_{c_m}^{rx}, \phi_c^{rx} + \phi_{c_m}^{rx}\right) \boldsymbol{e}_{tx}^H\left(\theta_c^{tx} + \theta_{c_m}^{tx}, \phi_c^{tx} + \phi_{c_m}^{tx}\right) \delta(\ell T_s - n_{c_m} T_s),$$

(3)

where $\ell = 0, 1, \ldots, L - 1$. Furthermore, P_{pl} indicates the pathloss between the transmitter and the receiver, while $\boldsymbol{e}_{tx}(\theta, \phi) \in \mathbb{C}^{N_B \times 1}$ and $\boldsymbol{e}_{rx}(\theta, \phi) \in \mathbb{C}^{N_U \times 1}$ denote the antenna array response vectors of the transmitter and the receiver, respectively. $\delta(t)$ is the Dirac function, T_s is the signaling time, and $n_{c_m} = \lfloor \frac{\tau_c + \tau_{c_m}}{T_s} \rfloor$.

The channel matrix at subcarrier k, denoted as $\mathcal{H}[k]$, can be written as $\mathcal{H}[k] = \sum_{\ell=0}^{L-1} \boldsymbol{H}[\ell] e^{-j\frac{2\pi k}{N_C}\ell}$. The overall Channel Frequency Response (CFR) matrix, denoted as $\mathbf{H}$, can be expressed as $\mathcal{H} = [\mathcal{H}[0], \mathcal{H}[1], \ldots, \mathcal{H}[N_C - 1]]$, where Nc is the number of subcarriers. This matrix is also known as the Channel State Information (CSI) and its estimation is referred to as the channel estimation problem.

The direct measurement of CSI is possible using MIMO-OFDM systems with fully digital beamforming which is available at sub-6 GHz bands. However, in the mmWave band, only analog beamforming is available, making direct CSI measurement not feasible. Instead, estimation techniques are used to obtain the CSI indirectly [47]. Channel estimation in mmWave massive MIMO channel is under extensive research and several CSI estimation methods have been proposed to this end [48–50]. Accurate estimation of these parameters is crucial for effective localization.

2.5 Angle-delay-profile (ADP)

Assuming a single antenna at the UE and a uniform linear array antenna at the BS, the ADP is a linear transformation of the CSI computed by multiplying it with two Discrete Fourier Transform (DFT) matrices $\boldsymbol{V} \in \mathbb{C}^{N_B \times N_B}$ and $\boldsymbol{F} \in \mathbb{C}^{N_C \times N_C}$. The ADP matrix $\boldsymbol{G} \in \mathbb{C}^{N_B \times N_C}$ is defined as follows [51]

$$\boldsymbol{G} = \boldsymbol{V}^H \mathcal{H} \boldsymbol{F},$$

(4)

where $\boldsymbol{V} \in \mathbb{C}^{N_B \times N_B}$ is defined as

$$[\boldsymbol{V}]_{i,k} \triangleq \frac{1}{\sqrt{N_B}} e^{-j2\pi \frac{\left(i\left(k - \frac{N_B}{2}\right)\right)}{N_B}},$$

(5)

and $\boldsymbol{F} \in \mathbb{C}^{N_C \times N_C}$ as

$$[\boldsymbol{F}]_{i,k} \triangleq \frac{1}{\sqrt{N_C}} e^{-j2\pi \frac{ik}{N_C}},$$

(6)

where $i = 0, \ldots, N_C - 1$ and $k = 0, \ldots, N_B - 1$.

This transformation has proven to be quite useful for various localization applications. **Figure 4** illustrates an example of the magnitude of the raw CSI $|\mathcal{H}|$ and its ADP transformation $|\boldsymbol{G}|$. The transformation converts the data into a sparse representation which has shown to improve the performance and generalizability of data-driven models [52]. Furthermore, in the visual representation of the raw CSI data, the scattering characteristics of the multipaths are ambiguous [53]. In contrast, the ADP
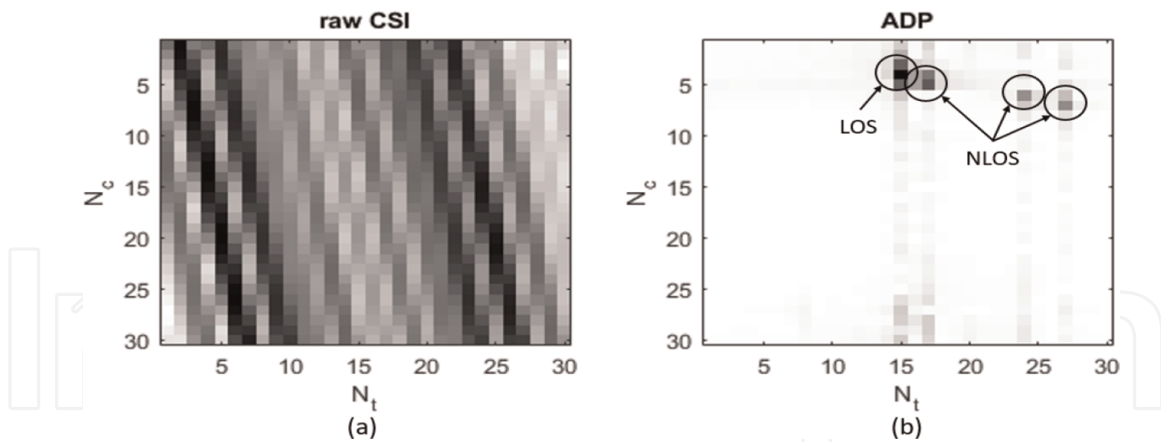
7

Figure 4.
(a) Raw CSI data of a OFDM-MIMO system with 30 sub-carriers. The BS is equipped with a uniform linear array antenna with 30 antenna elements, and UE with single antenna. (b) the ADP transformation of the CSI in (a) with LOS and NLOS path clusters labeled.

provides semantic visual interpretation of the channel multipath, where $[G]_{i,k}$ denotes the power of path associated with the angle

$$\theta_k = \arccos\left(\frac{2k - N_B}{N_B}\right), \tag{7}$$

and delay

$$\tau_i = iT_s. \tag{8}$$

The semantic visual interpretation means that the path clusters can easily be identified visually in the ADP. Referring to **Figure 4(b)**, the strongest peak in the ADP is the LOS path cluster and the remaining peaks are NLOS path clusters. This information is not visually observable in the raw CSI in **Figure 4(a)**.

2.6 Received signal strength indicator (RSSI)

The RSSI is a metric used in wireless communication systems that measures the strength of a received signal. RSSI parameters are typically used in distributed (or cell free) MIMO localization systems. Cell-free MIMO uses a large number of distributed antennas and MIMO techniques to improve coverage, capacity, and reliability compared to single-site MIMO system shown in **Figure 1**. Specifically, it aims to improve the performance of single-site MIMO systems by dynamically assigning antennas to users based on their location and available resources.

An example of a distributed MIMO system is illustrated in **Figure 5**. In this example, there are multiple BSs distributed in the environment. The RSSI is measured for each BS to create a RSSI vector $\mathbf{p} = (p_1, p_2, ..., p_M)$, where M represents the number of BSs and p_i is the RSSI from the ith BS. The RSSI vector should be unique for every location in the environment. To ensure the uniqueness of the RSSI vector, multiple BSs are necessary.

2.7 Channel parameters summary

The common channel parameters discussed above are summarized in **Table 1**. These parameters can be used individually or in combination to estimate the location
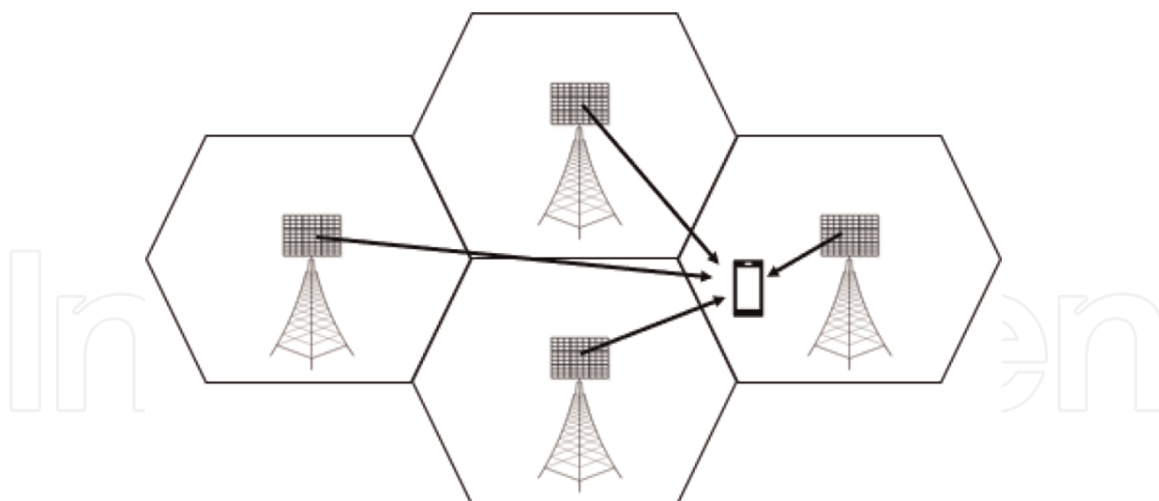
Figure 5.
Illustration of a distributed MIMO system with four BSs and one UE.

Parameter	Description	Notation
AoD	Angle-of-departure	$\left(\theta^{(t)}, \phi^{(t)}\right)$
AoA	Angle-of-arrival	$\left(\theta^{(r)}, \phi^{(r)}\right)$
ToA	Time-of-arrival (delay)	τ
CSI	Channel state information	$\mathbf{H}$
ADP	Angle delay profile	$\boldsymbol{G}$
RSSI	Received signal strength indicator	$\mathbf{p}$

Table 1.
List of MIMO channel parameters utilized in localization techniques.

of a UE. For instance, to define a propagation path, AoD or AoA is often used in conjunction with ToA.

3. Localization techniques

Localization is an extensive area of research in wireless MIMO communication and several different approaches have been proposed to solve this problem. This section provides an overview of the common localization techniques in sub-6 GHz and mmWave MIMO systems.

3.1 Map-assisted localization

Map-assisted localization techniques leverage 2D or 3D environment maps along with channel parameters to determine the location of UEs. The map provides information about the scattering surfaces and other obstacles in the environment. Then, by utilizing the AoD and delay of the signal path, multiple beam paths can be traced from the BS to the UE. This is illustrated in **Figure 6**. The paths are traced using the geometry defined in **Figure 2**. The point where these paths intersect is the UE's
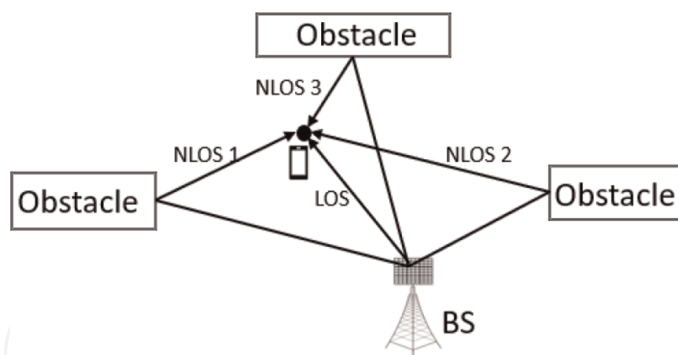
9

Figure 6.
Map-assisted localization using propagation path tracing. The figure illustrates the LOS path and three NLOS paths between the BS and UE. The intersection of these four paths represents the UE's location.

location. The minimum requirement to localize the UE is the AoD of two different paths. Alternatively, the UE can be localized if the angle and delay of a single path are known. The delay is used to estimate the length of the path by solving for d in (1). However, more precise localization is achieved by utilizing multiple paths and incorporating both angle and delay information. Furthermore, since the communication is bi-directional, either AoD or AoA can be used to estimate the UE's location.

When analog beamforming is available, which is typically at lower frequency bands (i.e. sub-6 GHz), the angle and delay can be directly measured. However, the mmWave bands digital beam forming is still prevalent, which does not enable measuring angle and delay directly. Therefore, angle and delay parameters have to be estimated. One approach to this problem is to estimate CSI and convert it to ADP. Then, the angle and delay can be estimated using (7) and (8), respectively.

3.2 Localization using compressive sensing techniques

Compressive Sensing (CS), also known as compressed sensing or sparse sampling, is a signal processing technique that allows for the reconstruction of a sparse signal from a small number of measurements or samples. CS has found its way in many applications [54, 55]. *Sparsity* is the property of a signal or data representation whereby a small number of coefficients or elements carry most of the signal's energy or information content, while the majority of coefficients or elements are zero or close to zero [56]. In fact, many real-world signals are sparse or compressible in either their original domain or some transform domain, such as Fourier or wavelet transforms [57]. An example is shown in **Figure 4**, where the raw CSI data is transformed into ADP to create a sparse representation. As may be observed in the ADP, the multipath components are concentrated into only a few clusters creating a sparse representation.

CS techniques have found many applications in wireless MIMO communication by exploiting the sparsity of channel model parameters [57, 58]. These applications include channel estimation, spectrum sensing, and localization. Channel estimation provides information on the AoA/AoD and ToA of the paths and thus the relative location of the UE with respect to the BS can be estimated.

In mmWave MIMO communication, channel estimation and localization are typically combined. The idea behind sparse channel estimation is that the system can make only a few random measurements which are then used to reconstruct channel model parameters using CS techniques. A commonly used CS technique in mmWave

MIMO channel estimation is Distributed Compressive Sensing - Simultaneous Orthogonal Matching Pursuit (DCS-SOMP). DCS-SOMP is typically used to estimate AoA/AoD and ToA [59–61]. Once the angle and delay channel parameters are recovered, the relative UE location can be estimated from the LOS path directly as shown in **Figure 2(a)**. When LOS is not available, the location can be estimated from the NLOS path by applying the virtual BS concept as shown in **Figure 2(b)**.

3.3 Fingerprinting-based localization

Fingerprinting is a data-driven localization technique that typically consists of two phases: offline phase and online phase. During the offline phase, the locations in the environment are mapped to a unique wireless measurement to create geo-tagged fingerprint database [62]. The unique wireless measurements are referred to as fingerprints. The measurements can be any wireless parameter such as RSSI, CSI/ADP, AoA/AoD or ToA. Then, during the online phase, the new measurement (fingerprint) is compared to the geo-tagged database to estimate the UE's location. The underlying principle behind fingerprinting is that the wireless channel between the UE and BS is uniquely determined by the scattering environment surrounding the UE's location [63]. Therefore, each location has a unique fingerprint. Matching a new wireless measurement to the measurements in the geo-tagged dataset typically involves a machine learning model. The training is performed during the offline phase. The most common fingerprinting models are based on Deep Learning (DL), Gaussian Progress Regression (GPR), or clustering and classification models.

RSSI-based fingerprinting is commonly used in wireless systems that have rich AP distributions such as Wireless Sensor Networks (WSNs) [64–66], Wi-Fi networks [67, 68], or Distributed Massive MIMO (DM-MIMO) systems [69, 70]. Since the RSSI provides a single measurement from the BS or AP, multiple APs are required to generate a unique fingerprint. On the other hand, single-site localization takes advantage of the multipath characteristics of the MIMO channel which are captured in CSI data or the angle and delay parameters that define the multipath. Furthermore, the CSI fingerprint can be used in its original form or it can be transformed into ADP.

3.3.1 Application of deep learning techniques

Deep Learning Neural Networks (DL NNs) require a large training dataset that covers the entire environment. The input to the NN is the wireless measurement and the output is the UE location. Several different NN architectures have been proposed in fingerprinting-based localization, including Multiple-Layer Perception (MLP) networks, [71, 72], Convolutional Neural Networks (CNNs), [51, 63, 73–75] and Recurrent Neural Networks (RNNs) [53].

Thus far, CNN models have demonstrated the highest localization accuracy performance. The CNN model treats the input fingerprint as a 2D image and performs series of convolutions over multiple layers to establish the spatial correlation in the 2D input. Typically, raw CSI or transformed ADP fingerprints are used for this application. The sparsity of ADP enhances the CNN model both from a computational complexity and a learning point-of-view [76]. RNN models are time series models that can track the changes of the input over time to predict the next UE location. RNN models can predict changes in the environment and account for these changes in the location estimation. RNN models are also used to predict the future location of the UE.
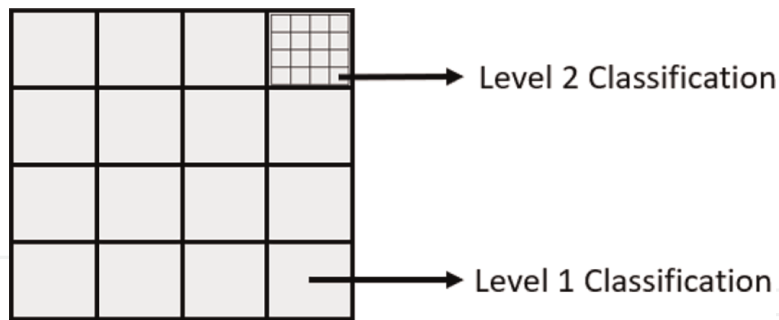
Figure 7.
Fingerprinting based multi-level classification grid of the environment map.

These networks can either be postulated as classification or regression models. In the classification models, the environment is usually divided into grids where each grid represents a class. If the area is larger, it is not uncommon to have multiple levels of classification, where each grid may be subdivided into smaller grids as shown in **Figure 7**. In general, the first level employs a CNN classification model (coarse search), whereas the second level utilizes a different machine learning algorithm to perform a fine search. In addition to increasing the complexity of the model, the multi-layer approach is more susceptible to errors. If at the first stage, the grid is classified incorrectly, then the error propagates into the second stage. Furthermore, the accuracy of the classification model is limited to the size of the grid. On the other hand, the goal of regression is to find a function or equation that best describes the relationship between the input and output variables. Therefore, regression models predict a continuous output variable and the accuracy is not limited to the grid as in classification.

3.3.2 Application of Gaussian process regression models

A *Gaussian Process* (GP) is a collection of random variable functions indexed by time or space. The key property of a GP is that any finite subset of the random variables is jointly Gaussian distributed. That is, for any finite set of vector elements $\mathbf{x}_1, \dots, \mathbf{x}_n \in \mathcal{X}$, the associated set of random variables $f(\mathbf{x}_1), \dots, f(\mathbf{x}_n)$ follow a joint Gaussian distribution. The following notation is commonly used in literature to represent the GP

$$f(\mathbf{x}) \sim \mathcal{GP}(m(\mathbf{x}), k(\mathbf{x}, \mathbf{x}')), \tag{9}$$

where the mean and covariance functions are defined as

$$m(\mathbf{x}) = \mathbb{E}[f(\mathbf{x})], \tag{10}$$

$$k(\mathbf{x}, \mathbf{x}') = \mathbb{E}[(f(\mathbf{x}) - m(\mathbf{x}))(f(\mathbf{x}') - m(\mathbf{x}'))] \tag{11}$$

for any $\mathbf{x}, \mathbf{x}' \in \mathcal{X}$ [77]. Therefore, the GP is entirely defined by its mean and covariance functions [78].

A Gaussian Process Regression (GPR) model is a non-parametric statistical model that uses a GP to model a continuous function and provides a probabilistic prediction with uncertainty estimates [79]. To define the GPR model, assume $\mathcal{D}_{train} \stackrel{\Delta}{=} (\mathbf{X}, \mathbf{y}) \stackrel{\Delta}{=} \{\mathbf{x}_i, y_i\}_{i=1}^n, \mathbf{x}_i \in \mathbb{R}^d, y_i \in \mathbb{R}$ to be an input–output pair training dataset. Furthermore,

assume that a latent function $f(\cdot)$ is responsible for generating the observed output y_i given the input vector $\mathbf{x}_i$. Then, GPR model can be defined as

$$y_i = f(\mathbf{x}_i) + \epsilon_i, \tag{12}$$

where $f(\mathbf{x}) \sim \mathcal{GP}(m(\mathbf{x}), k(\mathbf{x}, \mathbf{x}'))$, $\epsilon \sim \mathcal{N}(0, \sigma^2 \mathbf{I})$ is the noise of the system that has an independent, identically distributed (i.i.d.) Gaussian distribution with zero mean and variance σ^2, and i refers to the ith observation.

GPR models often assume zero mean as default. The correlation between input points is defined by the covariance function (also known as the kernel). There is a variety of kernels, including exponential, matern, quadratic, and more, each with hyper-parameters that can be fine-tuned during training [80]. Given a new testing sample $\mathbf{x}_*$, the mean and variance (uncertainty) of the unknown output $\mathbf{y}_*$ are predicted as

$$\overline{\mathbf{y}}_* = \mathbf{K}_*^{\mathbf{T}} \left(K + \sigma_n^2 I\right)^{-1} \mathbf{y}, \tag{13}$$

$$\mathbb{V}\left[\overline{\mathbf{y}}_*\right] = \mathbf{K}_{**} - \mathbf{K}_*^{\mathbf{T}} \left(K + \sigma_n^2 I\right)^{-1} \mathbf{K}_*, \tag{14}$$

where $\mathbf{K} = K(\mathbf{X}, \mathbf{X})$, $\mathbf{K}_* = K(\mathbf{X}, \mathbf{X}_*)$, and $\mathbf{K}_{**} = K(\mathbf{X}_*, \mathbf{X}_*)$ [81]. $\mathbf{K}$ is the covariance matrix (also known as Gram matrix) whose entries are the kernel functions $k(\mathbf{x}_i, \mathbf{x}_j)$ [79].

In localization, the objective of the GPR model is to define the latent function $f(\cdot)$ in (12), where $\mathbf{x}_i$ is the channel parameter (fingerprint) and y_i is the UE location. Given a new fingerprint $\mathbf{x}_*$, the UE location is predicted using (13), while the level of uncertainty in the prediction is estimated by (14). The fingerprint in distributed MIMO systems is usually the RSSI vector as proposed in [69, 70, 82]. On the other hand, the input in single-site MIMO systems can be AoA/AoD vector, CSI or ADP data as proposed in [83, 84].

The main advantage of GPR models over DL CNN models is that they can be trained on substantially smaller datasets. GPR models have shown the ability to train models with small-scale datasets due to the small number of hyper-parameters that define the model [84]. However, the GPR model does have its drawbacks. The main weakness of the GPR model lies in its training complexity, which is characterized by high computational and memory demands. Specifically, GPR training has a computational complexity of $O(n^3)$ and a memory complexity of $O(n^2)$, where n represents the number of training points in the dataset [85].

3.3.3 Clustering and classification

Clustering is a class machine learning algorithms used to group similar objects or data points together into clusters. The groupings are based on some similarity or distance measures. The goal of clustering is to identify patterns or structures in the data that may not be immediately apparent, and to group similar data points into clusters that can be easily analyzed or visualized. In localization, clustering techniques can be used to compare the test fingerprints to the fingerprints in the training database. K-means clustering and K-Nearest Neighbor (KNN) classification have widely been used in fingerprinting-based wireless localization and have shown to provide excellent accuracy given enough data point [86, 87]. The KNN location estimation is given by

$$\hat{p} = \frac{1}{K} \sum_{i=1}^{K} p_i, \tag{15}$$

Technique	Parameters	Methods
Map-Assisted	CSI/ADP	MAP-CSI [88]
	AoA and ToA	MAP-AT [91, 92]
CS	AoA/AoD	DC-SOMP [59–61]
Fingerprinting DL	CSI/ADP	MLP [71, 72, 93, 94], CNN [51, 73–75, 95], RNN [53]
	AoA	MLP [71]
	AoA and ToA	MLP [71]
	RSSI	MLP [71]
Fingerprinting GPR	CSI/ADP	GPR [83], FC-AE-GPR [84], DCGPR [96]
	RSSI	DM-MIMO [69, 70, 82, 97]
Fingerprinting clustering	CSI/ADP	KNN [51, 63, 86, 87, 93, 98]
	AoA	WMSE [90], ASCW [89]
	RSSI	KNN [99]

Table 2.
Methods in MIMO localization, categorized according to the localization technique employed and the parameters utilized.

where K is the number of surrounding neighbors considered and $\boldsymbol{p_i}$ is the coordinate of the ith nearest reference point. Weighted KNN (WKNN) is an extension of KNN where the contribution of each neighbor is weighted. The WKNN is defined as

$$\hat{\boldsymbol{p}} = \sum_{i=1}^{K} w_i \boldsymbol{p_i}, \qquad (16)$$

where w_i is the weight of the ith reference point. Typically, the weight corresponds to the distance between the reference point and the input point. The closer the neighbor is to the input point, the more weight it carries in the final prediction. The weights can also be defined by some similarity criteria calculated between the input and the reference fingerprint. Various similarity criteria have been established in wireless MIMO communication, such as normalized correlation [53, 86, 88], Joint Angle Delay Similarity Coefficient (JADSC) [63], Angular Similarity Coefficient Weight (ASCW) [89], and Weighted Mean Square Error (WMSE) [90].

3.4 Summary of methods

Table 2 provides a summary of the methods proposed in recent years that apply the localization techniques discussed in the previous subsection. The techniques are also grouped by the type of communication parameter used with the associated technique.

4. Challenges and opportunities

While MIMO systems offer many potential communication performance improvements and enable highly accurate localization models, several challenges still

need to be addressed. This section aims to introduce some of the main challenges in MIMO localization.

4.1 Dynamic environments

The majority of the models presented above assume a *static environment*, where the objects within the environment of interest are not moving or changing. In real world scenarios, we observe *dynamic environments* where objects are constantly moving through the environment changing the scattering in the environment quickly and thoroughly [53]. The static environment can be altered by any of the following dynamic changes:

- LOS blockage: a new object blocks the LOS path between the UE and the BS.

- NLOS blockage: a new object blocks some NLOS paths between the UE and the BS.

- NLOS addition: scattering from surfaces of a new object adds some NLOS paths between the UE and the BS.

Some efforts have been undertaken to mitigate the impact of dynamic changes. For example, through the analysis of the time sequence of fingerprints, it becomes possible to identify the moment when a dynamic change anomaly occurred. Models can then be developed to identify and remove the effect of the dynamic change anomaly from the fingerprint sample. However, countering the effects of the dynamic environment still poses a challenge in many proposed approaches.

4.2 Dataset collection

Data-driven localization techniques, specifically DL techniques, thus far have shown the best performance when it comes to accuracy. However, there is a major challenge with real world deployment of these models. In particular, data-driven methods necessitate extensive datasets for training the models, which are obtained through costly measurement campaigns that can be difficult to perform. Furthermore, as the environment changes, the dataset becomes invalid and a new measurement campaign needs to be deployed.

4.3 Generalization

Generalization in massive MIMO refers to the ability of a system to maintain good performance in a wide range of scenarios, including different channel conditions and new environments. This is important for practical deployment of massive MIMO systems, as it ensures that the system will work well in real-world environments where the conditions may vary.

Transfer Learning (TL) has been suggested as a potential approach to improve generalization in machine learning [73]. This technique involves reusing a pre-trained model to enhance the learning and generalization of a new model. In TL, the pre-trained model is fine-tuned to the new environment using a small dataset representative of that environment. The goal is to leverage the knowledge gained from the prior environment to enhance the learning and generalization of the new environment.

15

Some studies have been exploring TL techniques to adapt their models to new environments [73, 100, 101]. However, TL does not solve the problem completely as it still requires some data collection in new environments. Generalization remains an open area of research in DL-based localization.

4.4 Adversarial attacks

An adversarial attack is a type of cyber-attack where an attacker modifies data to deceive or harm a machine learning system, causing it to produce incorrect or unexpected results. DL techniques are vulnerable to such attacks, and intentional CSI perturbations can significantly impact the accuracy of fingerprinting-based localization. While few studies have addressed adversarial attacks and defenses in the context of MIMO systems [102], it remains an open area of research.

5. Conclusions

This chapter offers a comprehensive overview of the localization techniques proposed in wireless MIMO communication systems in sub-6 GHz and mmWave frequency bands. Initially, the need for highly accurate positioning systems is introduced along with some applications in LBS. Subsequently, the wireless communication parameters that define the propagation within the MIMO channel model are introduced. This is followed by a discussion on several localization techniques in MIMO systems including map-assisted, CS based, and fingerprinting models. This chapter explains how each localization technique uses wireless communication parameters to localize the UE. Finally, the last section outlines the remaining challenges and possible opportunities for improvement on MIMO localization.

Acknowledgements

Author details

Katarina Vuckovic*† and Nazanin Rahanvard†
University of Central Florida, Orlando, USA

*Address all correspondence to: kvuckovic@knights.ucf.edu

† These authors contributed equally.

IntechOpen

References

[1] Kenan M. Comparative analysis of localization techniques used in LBS. In: 2021 5th International Conference on Computing Methodologies and Communication (ICCMC). IEEE; 2021. pp. 300-304

[2] Djuknic GM, Richton RE. Geolocation and assisted GPS. Computer. 2001;**34**(2): 123-125

[3] Reed J, H, Krizman KJ, Woerner BD. An overview of the challenges and progress in meeting the e-911 requirement for location service. IEEE Communications Magazine. 1998;**36**:3037

[4] Majid Butt M, Rao A, Yoon D. RF fingerprinting and deep learning assisted UE positioning in 5G. In: 2020 IEEE 91st Vehicular Technology Conference (VTC2020-Spring). IEEE; 2020. pp. 1-7

[5] del Peral-Rosado JA, Raulefs R, López-Salcedo JA, Seco-Granados G. Survey of cellular mobile radio localization methods: From 1G to 5G. IEEE Communications Surveys Tutorials. 2018;**20**(2):1124-1148

[6] Kuutti S, Fallah S, Katsaros K, Dianati M, Mccullough F, Mouzakitis A. A survey of the state-of-the-art localization techniques and their potentials for autonomous vehicle applications. IEEE Internet of Things Journal. 2018;**5**(2):829-846

[7] Burghal D, Phadke G, Nair A, Wang R, Pan T, Algafis A, et al. Supervised learning approach for relative vehicle localization using V2V MIMO links. In: ICC 2022 - IEEE International Conference on Communications. IEEE; 2022. pp. 4528-4534

[8] Sarker MAL, Son W, Han DS. RIS-assisted hybrid beamforming and connected user vehicle localization for millimeter wave MIMO systems. Sensors. 2023;**23**(7)

[9] Wang H, Wan L, Dong M, Ota K, Wang X. Assistant vehicle localization based on three collaborative base stations via SBL-based robust DOA estimation. IEEE Internet of Things Journal. 2019;**6**(3):5766-5777

[10] Jia R, Kui X, Xia X, Xie W, Sha N, Guo W. Extrinsic information aided fingerprint localization of vehicles for cell-free massive MIMO-OFDM system. IEEE Open Journal of the Communications Society. 2022;**3**: 1810-1819

[11] Chen Y, Palacios J, González-Prelcic N, Shimizu T, Hongsheng L. Joint initial access and localization in millimeter wave vehicular networks: A hybrid model/data driven approach. In: 2022 IEEE 12th Sensor Array and Multichannel Signal Processing Workshop (SAM). Vol. 2022. IEEE. pp. 355-359

[12] Alexandropoulos GC, Vlachos E, Smida B. Joint localization and channel estimation for UAV-assisted millimeter wave communications. In: 2020 54th Asilomar Conference on Signals, Systems, and Computers. IEEE; 2020. pp. 1318-1322

[13] Rodriguez-Fernandez J, Gonzalez-Prelcic N, Heath RW. Position-aided compressive channel estimation and tracking for millimeter wave multi-user MIMO air-to-air communications. In: 2018 IEEE International Conference on Communications Workshops (ICC Workshops). Vol. 2018. IEEE; pp. 1-6

[14] Li X, Jie X. Positioning optimization for sum-rate maximization in UAV-

enabled interference channel. IEEE Signal Processing Letters. 2019;**26**(10): 1466-1470

[15] Bresson G, Alsayed Z, Li Y, Glaser S. Simultaneous localization and mapping: A survey of current trends in autonomous driving. IEEE Transactions on Intelligent Vehicles. 2017;**2**(3):194-220

[16] Placed JA, Strader J, Carrillo H, Atanasov N, Indelman V, Carlone L, et al. A survey on active simultaneous localization and mapping: State of the art and new frontiers. IEEE Transactions on Robotics. 2023;**39**:1-20

[17] Liu Y, Yujia F, Chen F, Goossens B, Tao W, Zhao H. Simultaneous localization and mapping related datasets: A comprehensive survey. arXiv preprint arXiv:2102.04036. 2021

[18] Zafari F, Gkelias A, Leung KK. A survey of indoor localization systems and technologies. IEEE Communications Surveys Tutorials. 2019;**21**(3):2568-2599

[19] Kim J, Hwangbo H, Kim SJ, Kim S. Location-based tracking data and customer movement pattern analysis for sustainable fashion business. Sustainability. 2019;**11**(22):6209

[20] Zhang D, Tan C. Application of indoor positioning technology in smart home management system. In: 2021 IEEE 2nd International Conference on Big Data, Artificial Intelligence and Internet of Things Engineering (ICBAIE). IEEE; 2021. pp. 627-631

[21] Snoonian D. Smart buildings. IEEE Spectrum. 2003;**40**(8):18-23

[22] Kehua S, Li J, Fu H. Smart city and the applications. In: 2011 International Conference on Electronics, Communications and Control (ICECC). IEEE; 2011. pp. 1028-1031

[23] Siano P. Demand response and smart grids—A survey. Renewable and Sustainable Energy Reviews. 2014;**30**: 461-478

[24] Chebrolu N, Lottes P, Läbe T, Stachniss C. Robot localization based on aerial images for precision agriculture tasks in crop fields. In: 2019 International Conference on Robotics and Automation (ICRA). IEEE; 2019. pp. 1787-1793

[25] Ding H, Zhang B, Zhou J, Yan Y, Tian G, Baoxing G. Recent developments and applications of simultaneous localization and mapping in agriculture. Journal of Field Robotics. 2022;**39**(6): 956-983

[26] Abouzar P, Michelson DG, Hamdi M. RSSI-based distributed self-localization for wireless sensor networks used in precision agriculture. IEEE Transactions on Wireless Communications. 2016;**15**(10): 6638-6650

[27] Mohanty MK, Thakurta PKG, Kar S. Efficient sensor node localization in precision agriculture: An ann based framework. Opsearch. 2023:1-24

[28] Mamehgol Yousefi DB, Mohd Rafie AS, Al-Haddad SAR, Azrad S. A systematic literature review on the use of deep learning in precision livestock detection and localization using unmanned aerial vehicles. IEEE Access. 2022;**10**:80071-80091

[29] Boccardi F, Heath RW, Lozano A, Marzetta TL, Popovski P. Five disruptive technology directions for 5G. IEEE Communications Magazine. 2014;**52**(2): 74-80

[30] Agiwal M, Roy A, Saxena N. Next generation 5G wireless networks: A comprehensive survey. IEEE

Communications Surveys & Tutorials. 2016;**18**(3):1617-1655

[31] Lu L, Li GY, Lee Swindlehurst A, Ashikhmin A, Zhang R. An overview of massive MIMO: Benefits and challenges. IEEE Journal of Selected Topics in Signal Processing. 2014;**8**(5):742-758

[32] Gao X, Edfors O, Rusek F, Tufvesson F. Massive MIMO performance evaluation based on measured propagation data. IEEE Transactions on Wireless Communications. 2015;**14**(7):3899-3911

[33] Payami S, Tufvesson F. Channel measurements and analysis for very large array systems at 2.6 GHz. In: 2012 6th European Conference on Antennas and Propagation (EUCAP). IEEE; 2012. pp. 433-437

[34] Ahmad T, Li XJ, Seet B-C. 3D localization using social network analysis for wireless sensor networks. In: 2018 IEEE 3rd International Conference on Communication and Information Systems (ICCIS). IEEE; 2018. pp. 88-92

[35] Bjornson E, Van der Perre L, Buzzi S, Larsson EG. Massive MIMO in sub-6 GHz and mmwave: Physical, practical, and use-case differences. IEEE Wireless Communications. 2019;**26**(2):100-108

[36] Chataut R, Akl R. Massive MIMO systems for 5g and beyond networks—Overview, recent trends, challenges, and future research direction. Sensors. 2020;**20**(10):2753

[37] Wang X, Kong L, Kong F, Qiu F, Xia M, Arnon S, et al. Millimeter wave communication: A comprehensive survey. IEEE Communications Surveys Tutorials. 2018;**20**(3):1616-1653

[38] Dan W, Wang J, Cai Y, Guizani M. Millimeter-wave multimedia communications: Challenges, methodology, and applications. IEEE Communications Magazine. 2015;**53**(1): 232-238

[39] mmMAGIC. Measurement Campaigns and Initial Channel Models for Preferred Suitable Frequency Ranges h2020-ict-671650-mmmagic/d2. 1 v1. 0. 2016

[40] Ali A, González-Prelcic N, Heath RW. Estimating millimeter wave channels using out-of-band measurements. In: 2016 Information Theory and Applications Workshop (ITA). IEEE; 2016. pp. 1-6

[41] Alrabeiah M, Alkhateeb A. Deep learning for mmwave beam and blockage prediction using sub-6 GHz channels. IEEE Transactions on Communications. 2020;**68**(9):5504-5518

[42] Sim MS, Lim Y-G, Park SH, Dai L, Chae C-B. Deep learning-based mmwave beam selection for 5G nr/6G with sub-6 GHz channel information: Algorithms and prototype validation. IEEE Access. 2020;**8**:51634-51646

[43] Shen Y, Win MZ. On the use of multipath geometry for wideband cooperative localization. In: GLOBECOM 2009 - 2009 IEEE Global Telecommunications Conference. IEEE; 2009. pp. 1-6

[44] Liu L, Oestges C, Poutanen J, Haneda K, Vainikainen P, Quitin F, et al. The COST 2100 MIMO channel model. IEEE Wireless Communications. 2012; **19**(6):92-99

[45] Ali A, González-Prelcic N, Heath RW. Millimeter wave beam-selection using out-of-band spatial information. IEEE Transactions on Wireless Communications. 2017;**17**(2): 1038-1052

[46] Alkhateeb A, Heath RW. Frequency selective hybrid precoding for limited feedback millimeter wave systems. IEEE Transactions on Communications. 2016;**64**(5):1801-1818

[47] Hassan K, Masarra M, Zwingelstein M, Dayoub I. Channel estimation techniques for millimeter-wave communication systems: Achievements and challenges. IEEE Open Journal of the Communications Society. 2020;**1**:1336-1363

[48] Dong P, Zhang H, Li GY, Gaspar IS, Alizadeh NN. Deep CNN-based channel estimation for mmWave massive MIMO systems. IEEE Journal of Selected Topics in Signal Processing. 2019;**13**(5): 989-1000

[49] Gao S, Dong P, Pan Z, Li GY. Deep learning based channel estimation for massive MIMO with mixed-resolution ADCs. IEEE Communications Letters. 2019;**23**(11):1989-1993

[50] Jin Y, Zhang J, Ai B, Zhang X. Channel estimation for mmWave massive MIMO with convolutional blind denoising network. IEEE Communications Letters. 2019;**24**(1):95-98

[51] Sun X, Chi W, Gao X, Li GY. Fingerprint-based localization for massive MIMO-OFDM system with deep convolutional neural networks. IEEE Transactions on Vehicular Technology. 2019;**68**(11):10846-10857

[52] Chen T, Zhang Z, Wang P, Balachandra S, Ma H, Wang Z, et al. Sparsity winning twice: better robust generalization from more efficient training. In: International Conference on Learning Representations. arXiv; 2022

[53] Hejazi F, Vuckovic K, Rahnavard N. DyLoc: Dynamic localization for massive MIMO using predictive recurrent neural networks. In: IEEE INFOCOM 2021 - IEEE Conference on Computer Communications. IEEE; 2021. pp. 1-9

[54] Shahrasbi B, Rahnavard N. Model-based nonuniform compressive sampling and recovery of natural images utilizing a wavelet-domain universal hidden Markov model. IEEE Transactions on Signal Processing. 1 Jan 2017;**65**(1):95-104. DOI: 10.1109/TSP.2016.2614654

[55] Tuan Nguyen M, Teague KA, Rahnavard N. CCS: Energy-efficient data collection in clustered wireless sensor networks utilizing block-wise compressive sensing. Computer Networks (IEEE). 2016;**106**:171-185

[56] Baraniuk RG. Compressive sensing [lecture notes]. IEEE Signal Processing Magazine. 2007;**24**(4):118-121

[57] Rani M, Dhok SB, Deshmukh RB. A systematic review of compressive sensing: Concepts, implementations and applications. IEEE Access. 2018;**6**: 4875-4894

[58] Gao Z, Dai L, Han S, Chih-Lin I, Wang Z, Hanzo L. Compressive sensing techniques for next-generation wireless communications. IEEE Wireless Communications. 2018;**25**(3):144-153

[59] Talvitie J, Valkama M, Destino G, Wymeersch H. Novel algorithms for high-accuracy joint position and orientation estimation in 5g mmwave systems. In: 2017 IEEE Globecom Workshops (GC Wkshps). IEEE; 2017. pp. 1-7

[60] Shahmansoori A, Garcia GE, Destino G, Seco-Granados G, Wymeersch H. Position and orientation estimation through millimeter-wave MIMO in 5G systems. IEEE Transactions on Wireless Communications. 2018;**17**(3):1822-1835

[61] Trivedi MA, van Wyk JH. Localization and tracking of high-speed trains using compressed sensing based 5G localization algorithms. In: 2021 IEEE 24th International Conference on Information Fusion (FUSION). IEEE; 2021. pp. 1-8

[62] Alamu O, Iyaomolere B, Abdulrahman A. An overview of massive MIMO localization techniques in wireless cellular networks: Recent advances and outlook. Ad Hoc Networks. 2021;**111**:102353

[63] Sun X, Gao X, Li GY, Han W. Single-site localization based on a new type of fingerprint for massive MIMO-OFDM systems. IEEE Transactions on Vehicular Technology. 2018;**67**(7):6134-6145

[64] Puckdeevongs A. Indoor Localization using RSSI and artificial neural network. In: 2021 9th International Electrical Engineering Congress (iEECON). IEEE; 2021. pp. 479-482

[65] Niu R, Vempaty A, Varshney PK. Received-signal-strength-based localization in wireless sensor networks. Proceedings of the IEEE. 2018;**106**(7): 1166-1182

[66] Csík D, Odry Á, Sarcevic P. Comparison of RSSI-based fingerprinting methods for indoor localization. In: 2022 IEEE 20th Jubilee International Symposium on Intelligent Systems and Informatics (SISY). IEEE; 2022. pp. 000273-000278

[67] Zhang G, Wang P, Chen H, Zhang L. Wireless indoor localization using convolutional neural network and gaussian process regression. Sensors. 2019;**19**(11):2508

[68] Lezama F, González GG, Larroca F, Capdehourat G. Indoor localization using graph neural networks. In: 2021 IEEE Urucon. IEEE; 2021. pp. 51-54

[69] Savic V, Larsson EG. Fingerprinting-based positioning in distributed massive MIMO systems. In: 2015 IEEE 82nd Vehicular Technology Conference (VTC2015-Fall). IEEE; 2015. pp. 1-5

[70] Moosavi SS, Fortier P. Fingerprinting localization method based on clustering and Gaussian process regression in distributed massive MIMO Systems. In: 2020 IEEE 31st annual international symposium on personal, Indoor and Mobile Radio Communications. Vol. 2020. IEEE. pp. 1-7

[71] Bhattacherjee U, Anjinappa CK, Smith LC, Ozturk E, Guvenc I. Localization with deep neural networks using mmwave ray tracing simulations. In: 2020 SoutheastCon. IEEE; 2020. pp. 1-8

[72] Decurninge A, Ordóñez LG, Ferrand P, Gaoning H, Bojie L, Wei Z, et al. CSI-based outdoor localization for massive MIMO: Experiments with a learning approach. In: 2018 15th International Symposium on Wireless Communication Systems (ISWCS). IEEE; 2018. pp. 1-6

[73] De Bast S, Guevara AP, Pollin S. CSI-based positioning in massive MIMO systems using convolutional neural networks. In: 2020 IEEE 91st Vehicular Technology Conference (VTC2020-Spring). IEEE; 2020. pp. 1-5

[74] Vieira J, Leitinger E, Sarajlic M, Li X, Tufvesson F. Deep convolutional neural networks for massive MIMO fingerprint-based positioning. In: 2017 IEEE 28th Annual International Symposium on Personal, Indoor, and Mobile Radio Communications (PIMRC). IEEE; 2017. pp. 1-6

[75] De Bast S, Guevara AP, Pollin S. CSI-based positioning in massive MIMO systems using convolutional neural networks. In: 2020 IEEE 91st Vehicular

Technology Conference (VTC2020-spring). IEEE; 2020. pp. 1-5

[76] LeCun Y, Bengio Y, Hinton G. Deep learning. Nature. 2015;**521**(7553):436-444

[77] Yiu S, Yang K. Gaussian process assisted fingerprinting localization. IEEE Internet of Things Journal. 2016;**3**(5): 683-690

[78] Görtler J, Kehlbeck R, Deussen O. A visual exploration of gaussian processes. Distill. 2019;**4**(4):e17

[79] Rasmussen CE, Williams CKI. Gaussian Processes for Machine Learning. Vol. 11. Cambridge, Massachusetts, USA: The MIT Press; 2005

[80] Duvenaud D. Automatic Model Construction with Gaussian Processes [Thesis]. Cambridge, UK: University of Cambridge; 2014

[81] Wang J. An Intuitive Tutorial to Gaussian Processes Regression. arXiv; 2021

[82] Prasad KNRSV, Hossain E, Bhargava VK. Machine learning methods for RSS-based user positioning in distributed massive mimo. IEEE Transactions on Wireless Communications. 2018;**17**(12): 8402-8417

[83] Moosavi SS, Fortier P. A fingerprint localization method in collocated massive MIMO-OFDM systems using clustering and Gaussian process regression. In: 2020 IEEE 92nd Vehicular Technology Conference (VTC2020-Fall). IEEE; 2020. pp. 1-5

[84] Vuckovic K, Hejazi F, Rahnavard N. CSI-Based Data-Driven Localization Frameworking Using Small-Scale Training Datasets in Single-Site MIMO Systems. arXiv; 2023

[85] Liu H, Ong Y-S, Shen X, Cai J. When Gaussian Process Meets Big Data: A Review of Scalable GPs. arXiv; 2018

[86] Qiu J, Kui X, Shen Z. Cooperative Fingerprint Positioning for Cell-free Massive MIMO Systems. Vol. 2020. 2020 International Conference on Wireless Communications and Signal Processing (WCSP). IEEE; pp. 382-387

[87] Wang X, Lin L, Lin Y, Chen X. A fast single-site fingerprint localization method in massive MIMO system. In: 2019 11th International Conference on Wireless Communications and Signal Processing (WCSP). IEEE; 2019. pp. 1-6

[88] Vuckovic K, Hejazi F, Rahnavard N. MAP-CSI: Single-site map-assisted localization using massive MIMO CSI. In: 2021 IEEE Global Communications Conference (GLOBECOM). IEEE; 2021. pp. 1-6

[89] Liao C, Xu K, Xia X, Xie W, Wang M. AOA-assisted fingerprint localization for cell-free massive MIMO system based on 3D multipath channel model. In: 2020 IEEE 6th International Conference on Computer and Communications (ICCC). IEEE; 2020. pp. 602-607

[90] Shen Z, Kui X, Xia X. 2D fingerprinting-based localization for mmwave cell-free massive MIMO systems. IEEE Communications Letters. 2021;**25**(11):3556-3560

[91] Kanhere O, Shihao J, Xing Y, Rappaport TS. Map-assisted millimeter wave localization for accurate position location. In: 2019 IEEE Global Communications Conference (GLOBECOM). IEEE; 2019. pp. 1-6

[92] Seow CK, Tan SY. Non-line-of-sight localization in multipath environments. IEEE Transactions on Mobile Computing. 2008;**7**(5):647-660

[93] Sobehy A, Renault É, Mühlethaler P. Generalization aspect of accurate machine learning models for CSI-based localization. Annals of Telecommunications. 2022;**77** (5-6):345-357

[94] Fan J, Chen S, Luo X, Zhang Y, Li GY. A machine learning approach for hierarchical localization based on multipath MIMO fingerprints. IEEE Communications Letters. 2019;**23**(10): 1765-1768

[95] Widmaier M, Arnold M, Dorner S, Cammerer S, ten Brink S. Towards practical indoor positioning based on massive MIMO systems. In: 2019 IEEE 90th Vehicular Technology Conference (VTC2019-Fall). 2019. pp. 1-6

[96] Wang X, Patil M, Yang C, Mao S, Patel PA. Deep convolutional Gaussian processes for mmwave outdoor localization. In: ICASSP 2021 - 2021 IEEE International Conference on Acoustics, Speech and Signal Processing (ICASSP). IEEE; 2021. pp. 8323-8327

[97] Walaa Y, Al-Rashdan, Tahat A. A comparative performance evaluation of machine learning algorithms for fingerprinting based localization in DM-MIMO wireless systems relying on big data techniques. IEEE Access (IEEE). 2020;**8**:109522-109534

[98] Sobehy A, Renault É, Mühlethaler P. CSI-MIMO: K-nearest neighbor applied to indoor localization. In: ICC 2020 - 2020 IEEE International Conference on Communications (ICC). IEEE; 2020. pp. 1-6

[99] René JE, Salazar A, Beltrán K, Caisaluisa O. Subscriber location in 5G mmwave networks - machine learning rf pattern matching. In: 2022 IEEE International Autumn Meeting on Power, Electronics and Computing (ROPEC). Vol. 6. IEEE; 2022. pp. 1-6

[100] Stahlke M, Feigl T, Castañeda García MH, Stirling-Gallacher RA, Seitz J, Mutschler C. Transfer learning to adapt 5G AI-based fingerprint localization across environments. In: 2022 IEEE 95th Vehicular Technology Conference: (VTC2022-Spring). IEEE; 2022. pp. 1-5

[101] Guo Z, Lin K, Chen X, Chit C-Y. Transfer learning for angle of arrivals estimation in massive MIMO system. In: 2022 IEEE/CIC International Conference on Communications in China (ICCC). IEEE; 2022. pp. 506-511

[102] Boora U, Wang X, Mao S. Robust massive MIMO localization using neural ODE in adversarial environments. In: ICC 2022 - IEEE International Conference on Communications. IEEE; 2022. pp. 4866-4871